

5.10 SIMILARITY OF DEEP VS. SHALLOW CONVECTION AS REVEALED BY A THREE-DIMENSIONAL CLOUD RESOLVING MODEL

Marat F. Khairoutdinov and David A. Randall

Department of Atmospheric Science, Colorado State University, Fort Collins, Colorado

1. INTRODUCTION

Cloud-Resolving Models (CRMs) have been used to study interactions among convective clouds, large-scale circulation and radiation, with the goal to evaluate and to improve the cloud parameterizations used in large-scale models. Consequently, the statistical properties of deep convection derived from CRM simulations have almost exclusively been limited to mean vertical profiles of convective mass fluxes, heating and moistening rates, primarily because those profiles could be compared in a rather straightforward manner to the output produced by single-column versions of general circulation models. However, to our knowledge, there has been no systematic CRM study of dynamical *similarity* of the statistical properties of deep convection and of the associated budgets of second moments such as kinetic energy, momentum fluxes, scalar fluxes, and variances, as routinely done, for example, in large-eddy simulation (LES) studies of boundary layer clouds.

2. MODEL AND SIMULATION

The results of this study are based on a 28-day long CRM simulation using the large-scale forcing derived from observations made during the ARM Summer 1997 IOP over the ARM SGP site in Oklahoma and Nebraska. The radiative heating rate is prescribed from the ECMWF estimates. We used a three-dimensional CRM/LES with the anelastic dynamical framework and bulk microphysics. A 3-D domain had $128 \times 128 \times 64$ grid points with $\Delta x = \Delta y = 2$ km and $100\text{m} < \Delta z < 500\text{m}$, with the top at 27 km. The time step was 10 sec. For this study, we identified five subperiods or convective events that produced hourly precipitation rates in excess of 10 mm/day for at least 5 consecutive hours (Figure 1). The events were from 5 to 15 hours long, with the event-mean precipitation rates in the range from 17 to 35 mm/day.

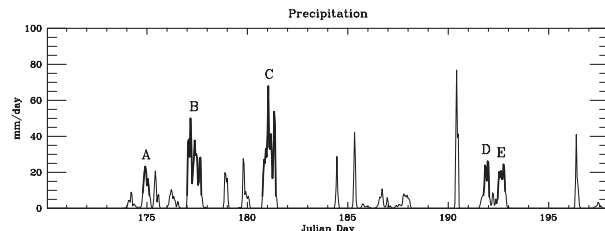


Figure 1: Time series of simulated hourly precipitation rate. The subperiods corresponding to the convective events used in this study are highlighted by thick lines.

Figure 2 shows the vertical profiles of some of the properties of the environment, large-scale forcing, and mean cloud statistics, while Figure 3 shows vertical profiles of several important dynamical characteristics averaged over each of the convective events.

3. SCALES AND SIMILARITY

Dynamic similarity among the simulated convective events is demonstrated using the following scaling parameters. The height is scaled by z_* defined as the height at which the buoyancy flux near the cloud top is most negative. The convective velocity scale, w_* , is

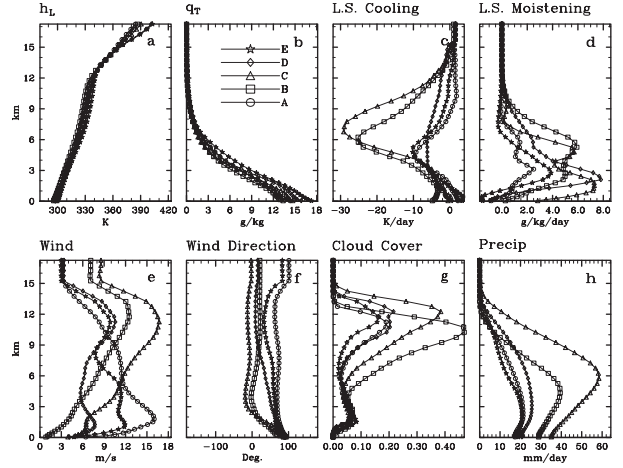


Figure 2: Profiles of the (a) liquid/ice water static energy, (b) total nonprecipitating water content, large-scale advective (c) cooling and (d) moistening tendencies, mean wind's (e) amplitude and (f) direction (counterclock from the west-east direction), (g) cloud fraction, and (h) precipitation flux for different convective events.

based on the vertically integrated buoyancy flux similar to definition used in the LES studies of stratocumulus-topped boundary layers. The temperature and total water scales are based on the vertical integrals of the corresponding fluxes.

$$w_*^3 = 2.5 \frac{g}{\Theta \rho_*} \int_0^{z_*} \overline{\rho w' \theta'_v} dz \quad (1)$$

$$\rho_* = \frac{1}{z_*} \int_0^{z_*} \overline{\rho} dz \quad (2)$$

$$T_* = \frac{1}{c_p \rho_* w_* z_*} \int_0^{z_*} \overline{\rho w' h'_L} dz \quad (3)$$

$$q_* = \frac{1}{\rho_* w_* z_*} \int_0^{z_*} \overline{\rho w' q'_T} dz \quad (4)$$

Event	A	B	C	D	E
z_* (km)	11.75	11.25	12.75	12.75	12.75
w_* (m/s)	2.20	2.98	4.49	2.91	2.07
ρ_* (kg/m ³)	0.55	0.58	0.53	0.55	0.54
T_* (K)	0.167	0.199	0.280	0.166	0.137
q_* ($\times 10^{-3}$ kg/kg)	0.062	0.081	0.108	0.071	0.055

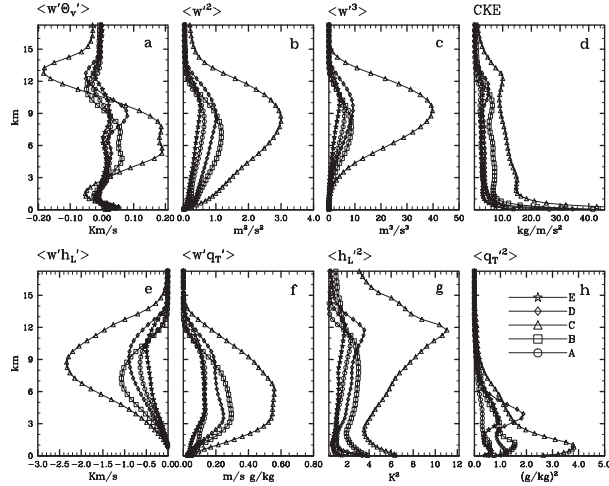


Figure 3: Profiles of the (a) buoyancy flux, (b) vertical velocity variance, (c) vertical velocity's third moment, (d) cumulus kinetic energy fluxes - (e) and (f) - and variances - (g) and (h) - of the liquid/ice water static energy and total nonprecipitating water, respectively, for different deep convective events.

Using these convective scales, we can make the profiles shown in Figure 3 dimensionless and plot them against dimensionless height as shown in Figure 4. One can see that there is quite a remarkable similarity among the simulated convective events in terms of the second-order moment statistics and the third moment of the vertical velocity.

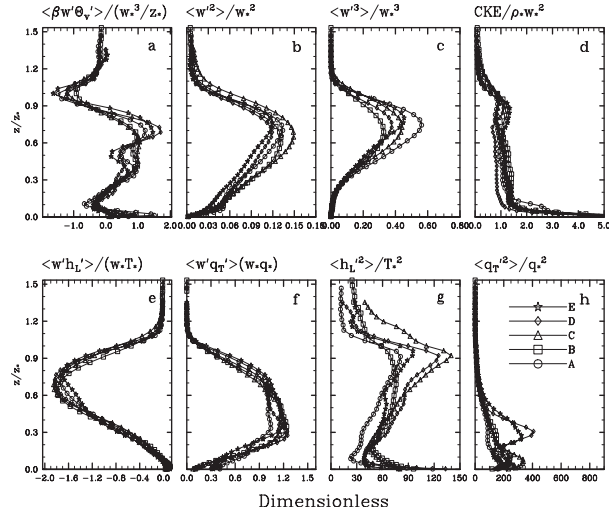


Figure 4: Same as Fig. 3, but made dimensionless for each convective event using convective scales (1)-(4).

In addition to the moments shown in Figure 4, the dimensionless budgets of several second moments such as convective kinetic energy (CKE, $= 0.5 \langle \rho \rangle \langle u_i' u_i' \rangle$), its vertical and horizontal components, variance and vertical flux of the prognostic thermodynamic variables, as well as momentum flux, are also shown to be similar. These budgets along with several triple correlations and budget of the vertically integrated CKE are discussed by Khairoutdinov and Randall (2002).

The most interesting aspect of the simulated CKE budget is that, above the PBL, the dissipation term is relatively small compared to the dominant buoyancy

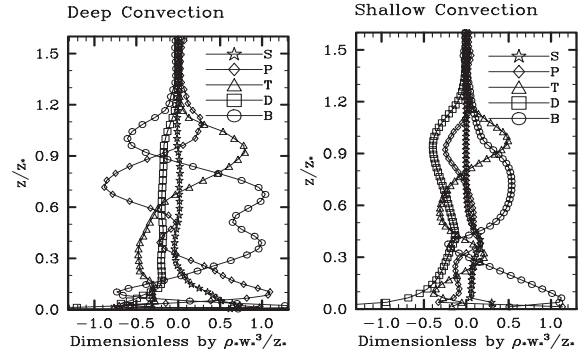


Figure 5: The comparison of the CKE budgets for deep (left) and shallow (right) convection. The deep convection budget is obtained by averaging the dimensionless CKE budgets for five ARM convective events. The shallow convection budget is obtained from the BOMEX trade-cumulus convection simulation. Symbols represent: S - shear production; P - pressure correlation; T - transport; D - dissipation; B - buoyancy production.

production, transport and pressure correlation terms. This makes the CKE budget in the case of deep convection differ from the CKE budget for the cloudy boundary layer and shallow trade-wind convection.

To illustrate this point, we conducted a simulation of shallow trade-cumulus convection forced by the Barbados Oceanographic and Meteorological Experiment (BOMEX) data as used by the GEWEX Cloud System Studies (GCSS) Working Group 1 for their LES model intercomparison project. The domain had $128 \times 128 \times 75$ grid-points and a uniform grid spacing of $\Delta x = \Delta y = 2.5 \Delta z = 100$ m. The model was run for 6 hours using 2 sec time step. The height scale, z_* , was defined as the height at which the advective transport term reaches its local maximum, where, presumably, most of the detrainment takes place. The other scales were defined using definitions (1)-(4). The scales were as follows: $z_* = 1540$ m, $w_* = 0.86$ m/s, $\rho_* = 1.1$ kg/m³, $T_* = 0.017$ K, and $q_* = 0.058$ g/kg. Figure 5 shows the composite (averaged over all five events) dimensionless CKE budget for deep convection versus a corresponding dimensionless budget for the shallow convection averaged over the last three simulated hours. One can see that, in contrast to the deep convection, the viscous dissipation plays a dominant role in the dynamics of shallow convection.

It is also found that the ratio of the vertically-integrated-CKE dissipation time scale to the eddy overturning time scale, z_*/w_* , is a factor 4-5 in the case of deep convection. In contrast, a similarly defined ratio in the case of simulated BOMEX shallow convection is found to be close to one.

Acknowledgments The authors thank Chris Bretherton and Peter Bechtold for very helpful comments and discussion. This research was supported in part by the U.S. Department of Energy Grant DE-FG03-95ER61968 to Colorado State University as part of the Atmospheric Radiation Measurement Program, and by National Science Foundation Grant ATM-9812384 to Colorado State University.

References

Khairoutdinov, M. F., and D. A. Randall, 2002: Similarity of deep continental cumulus convection as revealed by a three-dimensional cloud resolving model. *J. Atmos. Sci.*, in press.